

Preparation and Characterization of Chitosan-Coated Hydroxyapatite Nanoparticles as a Promising Non-Viral Vector for Gene Delivery

Jian-Wen Wang,¹ Ching-Yi Chen,² Yi-Ming Kuo¹

¹Department of Environmental and Safety Engineering, Chung Hua University of Medical Technology, 89 Wen-Hua 1st St, Jen-Te Hsiang, Tainan Hsien, Taiwan

²Department of Materials Science and Engineering, National Cheng Kung University, 1, Tainan 70101, Taiwan

Received 7 January 2010; accepted 10 January 2011

DOI 10.1002/app.34140

Published online 12 April 2011 in Wiley Online Library (wileyonlinelibrary.com).

ABSTRACT: Chitosan-coated hydroxyapatite (CS-HAp) nanoparticles have been prepared successfully by a modified dropping method. Variations of the final solution pH values, concentration of CS, and CS/HAp volume ratio were examined for their effects on particle size, intensity of surface charge, and tendency of particle formation. The smallest nanoparticles carry a positive charge with 40–50 nm in width and 60–70 nm can be obtained when the CS/HAp ratio is 1 by controlling the final solution pH value at 6.5. The ability of nanoparticles to complex DNA, toxicity of nanoparticles, and the effect of CS-HAp nanoparticle on transferring DNA were also investigated. Transgene

expression in HeLa and NIH3T3 cell on the nanoparticles were significant after 2 days. Agarose gel electrophoresis indicated a probable multiple interaction between DNA and CS-HAp while the interaction between DNA appears to be only ionic interaction. No toxic effect on the cells was seen with CS-HAp. Lipofectin, however, was observed to engender marked cytotoxicity. © 2011 Wiley Periodicals, Inc. *J Appl Polym Sci* 121: 3531–3540, 2011

Key words: chitosan; hydroxyapatite; biomaterials; nanocomposite; transfection

INTRODUCTION

Gene is a very unstable compound that needs to be protected from degradation in the biological environment. The development of appropriate vehicle to deliver new macromolecules coming out of the biotech industry is a meaningful challenge for pharmaceutical scientists. Generally, two different ways were developed for the delivering of nucleic acids in gene therapy, namely that of viral and nonviral vectors. Viral vectors are characterized by a high efficiency in introducing genetic materials. However, they develop a high immunogenicity after repeat administration, potential oncogenicity due to insertional mutagenesis, and the limited size of DNA that can be carried.¹ Nonviral system, especially polymer, shows significantly lower safety risks and can be tailored to specific therapeutic needs. They are capable of carrying large DNA molecules and can be easily produced in large quantities with a low cost.² The

major disadvantage of these nonviral vectors is their low transfection efficiency. Until now, we are still far away from a system that could be considered as satisfactory.

Cationic liposome, cationic polymers and dendrimers are the major types of nonviral gene delivery vectors.³ It has been observed⁴ that in addition to cytotoxicity, these carriers do not lead to satisfactory amount of gene expression in the cells. The reasons include (1) low endosomal escape, (2) no protection of DNA from nuclease degradation, and (3) inefficient nuclear uptake. It was envisaged that the use of inorganic nanoparticles, largely unexplored synthetic systems as vectors for gene delivery, might eliminate many of these limitations.

There are many good features of bioceramic nanoparticles that enable them to function as ideal DNA carriers.⁵ Calcium phosphate (CaP) microparticles and nanoparticles, silica (SiO₂) nanoparticles, inorganic nanorods, nanotubes, and other inorganic compounds have been developed as delivery systems and as adjuvant for DNA vaccines.⁶ Tan et al.⁷ indicated that protamine sulfate (PS), a FDA-approved USP compound for clinical use, was able to modulate effectively the surface charges of nanoparticles. The neutrally charged HA and negatively charged SiO₂ nanoparticles become positively charged thus allowing binding to the negatively charged DNA

Correspondence to: J.-W. Wang (jinwen.tw@yahoo.com.tw).

Contract grant sponsor: National Science Council of Taiwan, ROC; contract grant number: NSC-95-2221-E-273-007.

molecules through strong electrostatic interactions. Recently, Choy⁸ prepared inorganic layered double hydroxides (LDH) as nonviral vector. The high anion exchange capability of LDHs promotes their use as inorganic matrices for encapsulating functional charged biomolecules in aqueous media. Once bio-LDH hybrid is introduced into the cell, the hydroxide layers of Mg and Al are slowly removed from lysosomes under acid environment. Therefore, the use of a biocompatible surface modulating agent is a good way to enhance the transfection efficacies of the bioceramic nanoparticles.

Chitosan is a biological macromolecule extracted from the cuticle of marine crustaceans such as crabs and shrimps, and is made of glucosamine and *N*-acetylglucosamine units linked by 1–4 glycosidic bonds. Chitosan is a natural polycationic polymer that possesses useful properties such as high biocompatibility and nonantigenicity offering advantages for clinical uses.⁹ The hydrosoluble and positively charged properties enable chitosan to interact with polymers, bioceramic, and certain polyanions on contact in an aqueous environment. Chitosan also can open tight junctions between epithelial cells and facilitate the transport of macromolecules through well-organized epithelia. Therefore, chitosan-based colloidal delivery vehicles have been described for the association and delivery of macromolecules such as protein, antigens, and DNA.¹⁰ Since chitosan has a high affinity to cell membrane, several investigators have utilized chitosan derivatives as a coating agent for liposome, poly (lactide-*co*-glycolide) and polyepsilon-caprolactone. They found that by controlling the pH environment, polymer concentrations, mixing strategy, and prepared techniques (such as emulsion or solvent evaporation) a chitosan-coated nanocapsules or nanoparticles can be obtained.

The most ubiquitous form of CaP is HAp. This phase can be synthesized easily and has been studied extensively. As HAp has the advantage of adsorbability and high binding affinity with a variety of molecules, it has been used in various drug delivery systems, and used in separation, extraction, and purification of protein.¹¹ It is also one of the most stable phases that can be generated under physiological conditions; hence it has been the model system that has been commonly studied so far for nonviral gene delivery applications.¹²

HAp nanoparticles may be synthesized by a myriad of methods, including wet chemical methods, solid-state reactions, precipitation, hydrothermal reactions, and hydrolysis.¹³ Solid state reactions usually give a stoichiometric and well-crystallized product, but they require relatively high temperatures and long heat treatment times. The process for wet precipitated HA usually results in a fine-grained microstructure, even nano-to-submicron crystals.

Jarcho et al.¹⁴ have developed a precipitation process to prepare polycrystalline hydroxyapatite with the initial particles size of about 200 Å. As the sintered temperature increased to 1000°C, the size increased to 1500 Å. The low temperature processes such as hydrolysis of salts, electrochemical deposition, and sol-gel methods, etc. are hence very important in the synthesis of HA.¹⁵ Hydrolysis of tricalcium phosphate, monetite, brushite, or octacalcium phosphate requires low temperatures and results in HAp needles or blades having the size of submicrons.¹⁶ Therefore, it is a feasible way to obtain a nanocarrier by preparing HAp nanoparticle first then coating chitosan polymer on their surface.

The approaches to obtain CS-HAp composite materials are based either on mixing or coprecipitation methods. Beppu et al.¹⁷ employ either the biomineralization of CS in a solid form in simulated body fluids or by mixing of a CS solution with different CaPs fillers followed by their precipitation as hydrogel composite. Yamaguchi et al.¹⁸ have developed one of the coprecipitation methods that lead to a type of CS-HAp composites. Rusu et al.¹⁹ have reported a stepwise coprecipitation method in which the pH of the CS solution is gradually increased in a stepwise fashion. They indicated that the average HAp crystallite size can be controlled by varying the pH and dynamic operation condition and/or by varying the weight proportions of CS to inorganic ion concentration conditions. Recently, Willson Jr et al.²⁰ reported that chitosan exhibits strong adsorption interactions with HAp and enhances colloid stability for processing of CS-HAp nanocomposites. They also found that acetic acid did not decompose synthetic hydroxyapatite during solution processes. Based on those ideas, a combined method to synthesis CS-HAp nanoparticle was proposed in this study. First, nanosized HAp was prepared by hydrolysis of brushite at low temperature. Then CS-HAp nanoparticle was obtained by stepwise dropping nanosized HAp into CS solution. CS-HAp size is controlled by varying the pH and the volume ratio of CS to HAp. The relevance between transfection efficiency and CS-HAp-DNA nanoparticle will be discussed. The specific points, including the approach to obtain smaller nanoparticle size, the suitable nanoparticle size interacting with DNA to form a smaller nanoparticle, and the nanoparticle size performed in different gene expressions.

EXPERIMENTAL

Materials

Chitosan (CS, $M_w = 40,000$) was purchased from Fluka biochemical (USA). The degree of deacetylation (DD) was about 88% determined by IR method.

Dicalcium phosphate dihydrate ($\text{CaHPO}_4 \cdot 2\text{H}_2\text{O}$, DCPD) (purity 98%) was supplied by Riedel-de Haën (Germany). NaOH was supplied by Showa (Japan). Acetic acid was obtained from Fluka (USA). All other reagents were of analytical grade and used without further purification.

Synthesis of nanosized HAp

Nanosized HAp particles were prepared by a hydrolysis technique based on the procedure of Shih et al.²¹ In a typical reaction, the raw material powders of DCPD with Ca/P = 1.5 were mixed and added to 500 mL of 10 wt % NaOH (pH = 13) with high-speed thermostatic agitation at 75°C for 1 h. The reaction was terminated by cooling in ice water. The solution was filtered, washed, and dried at 60°C for use. Since DCPD has low solubility in water, this hydrolysis process is a fast solid phase reaction under high pH and temperature over 60°C and the solubility of the mixture are less important.²²

Synthesis CS-HAp nanoparticle

Chitosan solutions were made at 1, 2, 3, 4, and 5 wt % using chitosan, acetic acid, and deionized water. The wt % corresponded to both chitosan and acetic acid concentrations. The CS solutions were prepared by dispersing the chitosan into the aqueous acetic acid solution and allowing the chitosan to dissolve over a 4-h time period. The HAp suspensions were prepared at a concentration of 1 wt %. The HAp suspensions were dropped into chitosan solution in a volume ratio of 2 : 1, 1 : 1, and 1 : 2 at a dropping rate of 1 drop s^{-1} using a syringe connected to a peristaltic pump. The final pH value of the reaction suspensions was adjusted to pH 6.5, 7.4, and 10.5 by adding 10 wt % NaOH. The samples were washed a minimum of three times with deionized water and dried at room temperature for further analysis.

The loading of DNA on CS-HAp nanoparticles

CS-HAp nanoparticles were washed and suspended in 500 mL of 10 mM Tris buffer pH 7.0. A sterilized phosphate buffered saline (PBS, pH 7.4) containing pEGFP-N₂ plasmid (200 $\mu\text{g mL}^{-1}$) through a syringe filter for sterilization was added gradually to the nanoparticles suspension (1 mg mL^{-1}) and vortexed. The mixture was incubated for 1 h at 37°C water bath to allow the complete formation of polyplexes. The CS-HAp:DNA ($\mu\text{g } \mu\text{g}^{-1}$) was controlled with the ratio of 0.1 : 1, 0.2 : 1, 0.5 : 1, 1 : 1, 2 : 1, and 4 : 1. Polyplexes were produced at a constant DNA concentration of 20 $\mu\text{g mL}^{-1}$ for gel retarding analysis and transfection experiment.

Characterization

CS-HAp nanoparticles were characterized by FTIR-ATR, XRD, TEM, BET, and Zetasizer analysis. FTIR-ATR spectra were measured with a Thermo Nicolet (Madison, WI) Nexus 470 FTIR-ATR spectrometer to determine the chemical interaction between CS and HAp. The spectra were collected from 4000 to 400 cm^{-1} with a 4- cm^{-1} resolution over 40 scans. The crystal structure of the CS-HAp nanostructure was observed using an X-ray diffractometer (Rigaku, Japan) at a scanning rate of 4°/min for 2 θ from 10° to 50° with a CuK R X-ray source. The quantitative analyses on the crystallinity of the nanoparticles were performed using a multipeak separation program (MDI Jade 5.0, Materials Data, Livermore, CA). The fraction of crystalline apatite phase in the investigated volume of nanopowder was determined upon using the (0 0 2) reflection peak.^{19,23} A Hitachi HF-2000 field emission transmission electron microscope (Tokyo, Japan) was used to observe the morphology of the nanoparticles. The samples were placed on a copper film at room temperature without staining. The Malvern Zetasizer 3000HS (Herrenberg, Germany) was used to determine the size distribution and zeta potential of the nanoparticles at 25°C. The size distribution obtained from photon correlation spectroscopy (PCS) is based on the intensity of scattered light. PCS, also known as dynamic light scattering (DLS), relies on the measurement of the movement of particles undergoing Brownian motion. The size distribution will therefore differ from the values obtained by other techniques, e.g., electron microscopy. The intensity distributions can be converted to volume and number distributions.²⁴ Each sample of the nanoparticles suspension was adjusted to a concentration of 0.01 wt % in deionized water, or in 0.01M sodium chloride solution in the case of zeta potential examination. All analyses were triplicated and the results are the average of three runs. The specific surface area of the chitosan-modified HAp was determined by BET apparatus N₂ adsorption using a Micromeritics ASAP 2010 system (Norcross, GA).

Gel retarding analysis

Coupling ability of CS-HAp nanoparticles for plasmid DNA pEGFP was evaluated by agarose gel electrophoresis. The Polyplexes prepared with CS-HAp of various weight ratios (CS-HAp:DNA ($\mu\text{g } \mu\text{g}^{-1}$) was controlled with the ratio of 0.1 : 1, 0.2 : 1, 0.5 : 1, 1 : 1, 2 : 1, and 4 : 1) and the naked plasmid was loaded onto a 0.8% w/v agarose gel. The samples were run on the gel at 80 V for 60 min; then the gel was stained with ethidium bromide and photographed using an UV illuminator (Eagle EyeP,

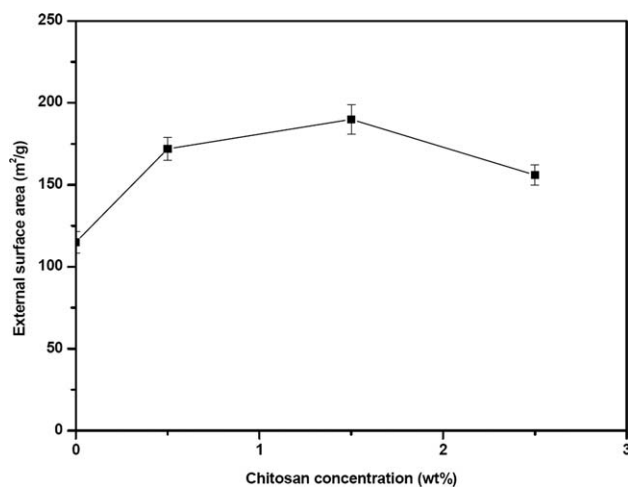


Figure 1 BET Nitrogen adsorption data showing the influence of HAp in CS gel on specific surface area as a function of increasing chitosan concentration (preparation conditions: CS/HAp with a volume ratio of 1 : 1).

Stratagene, La Jolla, CA) to document the mobility of the DNA.

Biocompatibility of CS-HAp nanoparticles

Cytotoxicity studies were performed by NIH3T3 cell line and HeLa cell line. HeLa and NIH3T3 cells were seeded at a density of 1×10^4 cells per well in 100 μ L growth medium in 96-well plates and grown overnight. Immediately after growth medium was removed, the cells were immediately treated with various doses (10, 20, 30, 40 μ g) of CS-HAp nanoparticles for another 8 h. Cells treated with fresh culture media only were used as control. Incubation was performed for 8 h before removal of media containing complexes and replacement with fresh culture media. After 24 h, 100 μ L MTT solution (5 mg mL⁻¹ in PBS) was added, and the cells were incubated for additional 4 h at 37°C for MTT formazan formation. Then, the MTT containing medium was replaced with 200 μ L of isopropanol-HCl (0.1N) and kept at 37°C for 10 min to solubilize the formazan crystals. The samples were transferred to 96-well plates and the absorbance of the converted dye was measured at 570 nm. The percent cell viability of the control cells was taken as 100%.

In vitro transfection studies using HeLa and NIH3T3 cell lines

For *in vitro* study, HeLa cells and NIH3T3 cells are maintained in DMEM of pH value 7.4, supplemented with 1% (w/v) nonessential amino acids, 10% (v/v) fetal calf serum (FCS), benzyl-penicillin G and streptomycin sulfate. The cells are seeded on 24-well plates at a seeding density of 10^5 cells/well and cultured at 37°C in a humidified atmosphere of

5% CO₂ and 95% air for 24 h prior to transfection. When the cells were at 80–90% confluence, the culture medium was replaced with 200 μ L serum-free medium containing definite volumes of complexes (10, 20, and 30 μ L of CS-HAp/DNA complexes). pEGFP-N₂ was used as the reporter plasmid to assay the transfection efficiency. Lipofectin was used as a positive control according to the manufacturer's procedures. Naked DNA was used as a negative control. After incubation for 6 h at 37°C in a 5% CO₂ incubator, the cells received 1 mL of complete medium and incubated sequentially until 40 h post transfection. The transfection efficiency of the cells was estimated by flow cytometry. For flow cytometry, HeLa and NIH3T3 cells after being transfected with pEGFP-N₂ were washed with PBS and trypsinized. Transfection efficiency was evaluated by scoring the percentage of cells expressing green fluorescence protein using a FACS Calibur System from Becton-Dickinson. The experiments were performed in triplicates and 1×10^5 cells were counted in each experiment.

RESULTS AND DISCUSSION

The influence of chitosan concentration on the surface chemistry of HAp

Chitosan exhibited a strong adsorption behavior on HAp particles improving their colloid stability.²¹ According to our preliminary study, CS-HAp nanocluster can be formed instantly by dropping HAp solution (1 g HAp dissolved in 100 mL deionized water) into CS solution (1 g CS dissolved in diluting acetic solution) in a volume ratio of 1 : 1 without pH adjustment. In this study, CS-HAp suspensions were prepared by mixing 10 g of 1, 2, 3, 4, and 5 wt % CS with an equal mass (10 g) of an aqueous HAp suspension containing 1 wt % HAp in a volume ratio of 1 : 1 without pH adjustment. The final sample contained 0.5 g of HAp in 0.5 wt % CS, 1 wt % CS, 1.5 wt %, 2 wt % CS, and 2.5 wt % CS. To obtain a stable and high specific area of nanoparticle, the influence of chitosan concentration on the surface chemistry of HAp was evaluated firstly by BET N₂ adsorption.

Figure 1 shows the chitosan addition influenced the specific surface area of HAp. The specific surface area of HAp increased as a result of chitosan addition increased. HAp had a specific surface area of 115 m² g⁻¹. The specific surface area of CS-HAp increased as chitosan concentration increased before 1.5 wt % and reached a maximum of 190 m² g⁻¹. However, the specific surface area of CS-HAp decreased as chitosan concentration more than 1.5 wt %. According to the study of Wu and Bose,²⁵ once the concentration of surfactant reached the CMC (critical micelle concentration), the micelle

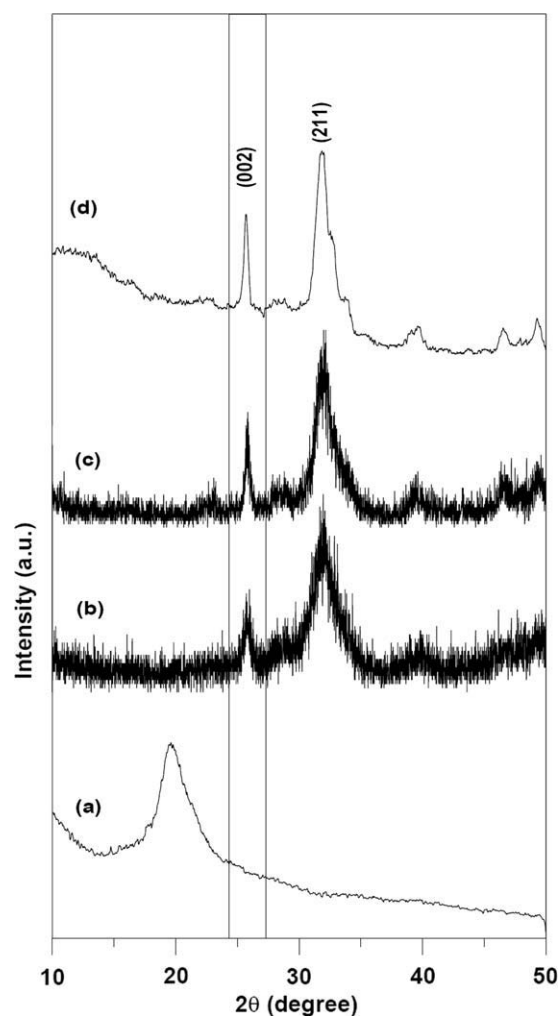


Figure 2 XRD patterns of the (a) CS (b) CS-HAp nanoparticle prepared at pH 6.5 (c) CS-HAp nanoparticle prepared at pH 10.5 (d) nano-sized HAp (preparation conditions: CS/HAp with a volume ratio of 1 : 1, final sample contain 1.5 wt % CS).

formed, which acted as a template for the HAp precipitate and provided the highest surface area in the final powders. In this study, chitosan can be as a cationic surfactant. Therefore, a 1.5wt % CS concentration gave the highest surface area in the final HAp powder. However, as the concentration of surfactant gets above CMC, the size of micelles increases with the increase of surfactant concentration. At higher concentrations (CS concentration more than 1.5 wt %), the micelles are strongly adsorbed and the charged HAp acts, at least in part,

as the counter ion for the chitosan. The presence of strong electrostatic attraction between the micelles and the charged HAp may promote bridging phenomena between different particles. Therefore, the particle agglomeration will occur at high concentration results in lower specific average surface area.²⁶ Chitosan-coated particles have been proposed for biomacromolecule delivery. However, like other cationic polymers, the strong positive charge of chitosan contributes to the toxicity of the polymer. The amount of chitosan can be substantially decreased by making chitosan-coated HAp, because only a lower amount of chitosan was expected to coat on the surface of a particle compared to free chitosan. This is particularly true due to the large surface-to-volume ratio of the particles that were produced. Therefore, the chitosan concentration was fixed at 1.5 wt % for further study.

Effect of pH value on the formation of CS-HAp nanoparticle

Crystallinity of CS-HAp nanoparticle

According to Yamaguchi et al.'s study,²⁷ in using solution processes to make HAp/CS composites, HAp is introduced into an acidic environment that can influence its solubility and surface chemistry and phase stability. Therefore, the influence of pH value on the formation of CS-HAp nanoparticle was first studied by XRD analysis. The XRD pattern was verified by the powder diffraction file.

Figure 2 shows XRD patterns of nanosized HAp crystals and CS-HAp nanoparticle prepared by different pH condition. All the samples were of typical apatite crystal structure but have different crystallinity with respect to phase composition. The XRD pattern of nanosized HAp shows a broad peak with poor crystallinity around $2\theta = 32^\circ$. The poor crystalline nature of nanosized HAp was emerged from the preparation process owing to low temperature procedure.²⁸ The obtained results did not show any peaks corresponding to dicalcium phosphate dihydrate and hence suggesting that the dicalcium phosphate dihydrate was reacted completely by the hydrothermal method and produced a homogeneous HAp. Table I also shows that the adsorption of chitosan on HAp decreases the crystallinity of HAp. We can conclude that this is due to the electrostatic

TABLE I
Fraction Crystallinity of Nanosized HAp and CS-HAp Nanoparticle Prepared at Different pH Values

Sample	Plane	Line width FWHM ($^\circ$)	Fraction crystallinity
CS-HAp nanoparticle prepared at pH 6.5	(0 0 2)	0.485	0.133
CS-HAp nanoparticle prepared at pH 10.5	(0 0 2)	0.432	0.145
Nano-sized HAp	(0 0 2)	0.321	0.402

TABLE II
Mean Particle Size and Zeta Potential of CS-HAp Nanoparticles at Different CS/HAp Volume Ratios and pH Values

Sample no.	pH value	CS : HAp (v : v)	Mean diameter (nm)	Polydispersity	Zeta potential (mv)
I	6.5	1 : 2	55 ± 3	0.0304	26.2 ± 0.2
II	6.5	1 : 1	68 ± 2	0.0583	33.1 ± 0.4
III	6.5	2 : 1	88 ± 7	0.0601	35.5 ± 0.7
IV	7.4	1 : 1	115 ± 12	0.1841	18.4 ± 0.3
V	10.5	1 : 1	— ^a	— ^a	— ^a

^a Aggregated.

Prepared condition: mixing 10 g of 3 wt % CS with 10 g of an aqueous HAp solution containing 1 wt % Hap.

repulsion and expect that such a crystalline order would depend on pH.

Mean diameter and morphology of CS-HAp nanoparticles

Table II shows the results of the mean diameter and surface charge of the CS-HAp nanoparticles with the CS/HAp volume ratio fixed at 1 under different pH values. It can be seen that the diameter of the nanoparticles increased with increasing pH value from 6.5 to 7.4, but aggregated at final pH value equal to 10.5. In addition, the surface charge of nanoparticles decreased as pH value increased. The increase in measured average particle size could have been caused mainly by particle aggregation when the solution pH value increased. The increase in size at pH 7.4 suggested that the degree of protonation at the surfaces of the particles was reduced, which decreased the electrostatic repulsion between the particles and, thereby, increased the probability of particle aggregation. TEM images [Fig. 3(a)] also show that as the final pH value of CS-HAp solution is equal to 6.5, a rod-like nanoparticles can be obtained with 40–50 nm in width and 60–70 nm in length. However, as the final pH value of CS-HAp suspension is equal to 10.5 [Fig. 3(b)], CS-HAp membranes are formed and aggregated seriously. It may be due to the reason that under extremely basic solution, almost all amine groups from CS were in the form of NH_2 resulted in an aggregation of CS-HAp particles.

Effect of CS/HAp volume ratio on the mean diameter and morphology of CS-HAp nanoparticles

The mean particle size of CS-HAp nanoparticles, prepared by a precipitated method with various CS/HAp volume ratios was characterized by Zetasizer at pH 6.5. It is shown that the diameter of each sample is smaller than 100 nm. With increasing CS/HAp volume ratio, the mean size of the nanoparticles increased. The surfaces of the CS-HAp nanoparticles had positive charges of about 20–40 mV due to the cationic characteristic of CS. Table II also

shows that as the volume ratio of CS/HAp increased, the zeta potential also increased. As the content of CS exceeded that of HAp, some of the excessive CS was absorbed onto the surface of the CS-HAp nanoparticles. The excess CS increased the surface charges of the CS-HAp nanoparticles and

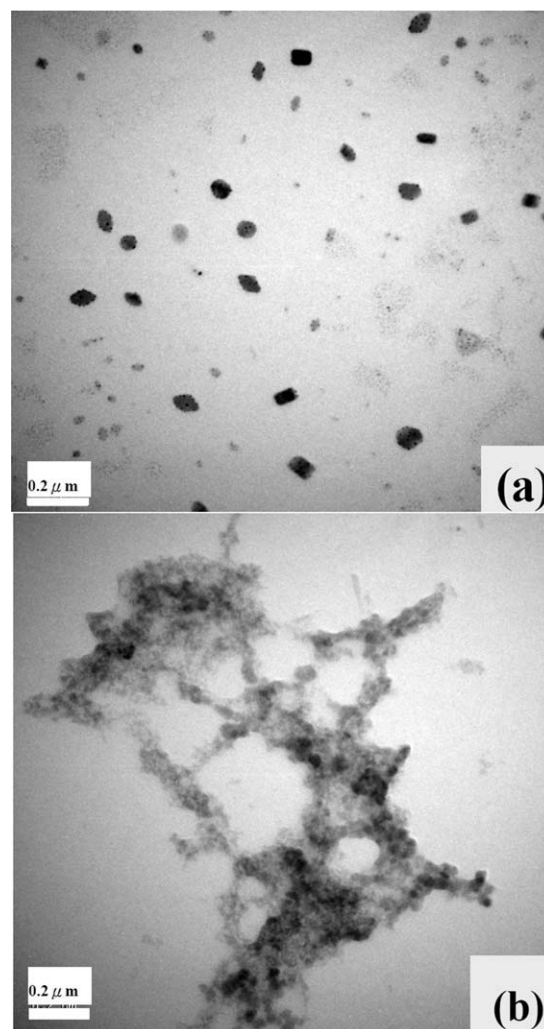


Figure 3 TEM images of CS-HAp nanoparticles prepared at different pH condition (a) 6.5 (b) 10.5 (preparation conditions: CS/HAp with a volume ratio of 1 : 1, final sample contain 1.5 wt % CS).

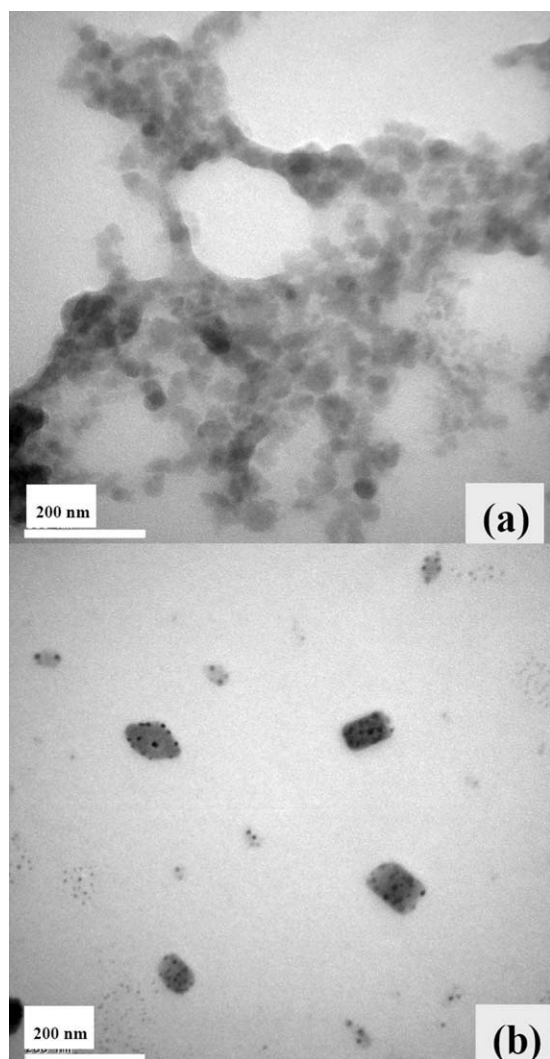


Figure 4 TEM images of CS-HAp nanoparticles prepared with CS/HAp in a volume ratios of (a) 1 : 2, (b) 1 : 1 (preparation conditions: pH = 6.5).

resulted in an increase in the zeta potential. TEM images of the CS-HAp nanoparticles prepared by different CS/HAp volume ratios were also shown in Figure 4. As shown in Figure 4(a), the agglomeration of CS-HAp nanoparticles in the volume ratio of 1 : 2 is observed. It may be due to some uncoated adjacent nano-sized HAp particle aggregated.²⁹ However, with increasing CS/HAp volume ratio, rod-like particle is significantly dispersed with 40–50 nm in width and 60–70 nm in length [Fig. 4(b)]. These findings are consistent with the results of a study by Yamaguchi et al.²⁷ At the HAp-rich region, the chitosan molecules were covered with HAp crystals as interaction. Therefore, agglomeration of CS-HAp nanoparticles is observed. At the chitosan-rich region, the surface of CS-HAp nanoparticles was covered with chitosan molecules, those molecules caused the CS-HAp nanoparticles to be homogeneous.

Intermolecular interaction between the components

The FTIR-ATR spectrum of nano-sized HAp, CS, and CS-HAp nanoparticle (prepared with CS/HAp = 1 at pH 6.5) is shown in Figure 5. The CS-HAp composite is characterized by absorption bands arising from HAp and CS. The absorption bands observed at 1665 and 1580 cm^{-1} were assigned to amide I (C=O) and amide II (NH–) in chitosan, respectively. The basic characteristics of CS at 3450 cm^{-1} (OH stretching and N–H stretching) and 2920 cm^{-1} (C–H stretching on methyl) also can be observed. The absorption bands at 3750 and 1025 cm^{-1} are attributed to the OH and phosphate groups of HAp. Those bands at 603 and 563 cm^{-1} are due to phosphate bending vibration. For CS-HAp nanoparticles, the two characteristic peaks of CS decrease dramatically. The shift of the characteristic bands of the protonated amine and phosphate to the lower wave number (1380, 1560, and 1650) in CS-HAp was observed in Figure 5(a) for the functional group of chitosan, and may be attributed to interactions involving these groups. The FTIR data suggest that there is an association between chitosan and the phosphate ions that may be cross-linking the chitosan chains.

Modulation of the surface charge of the HAp nanoparticles to optimize DNA binding

It is difficult for naked DNA to cross the nuclear membrane pore into the nucleus where transgene

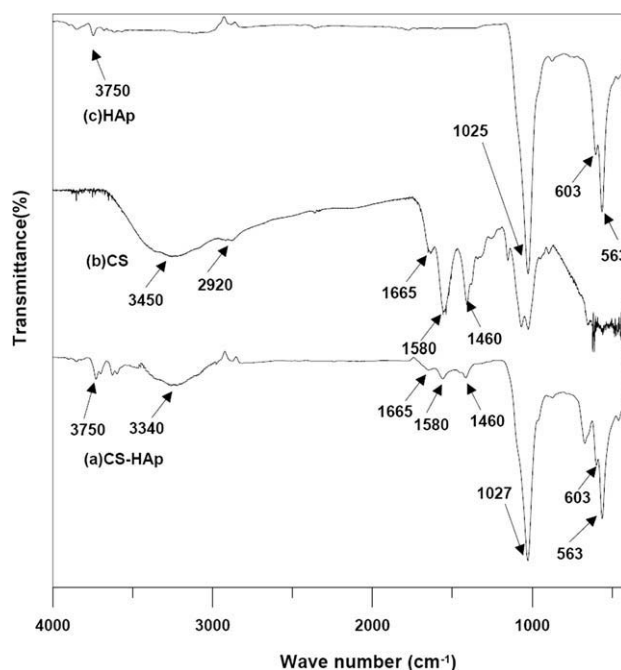


Figure 5 FTIR-ATR spectrum of (a) CS-HAp nanoparticle (b) CS and (c) nano-sized HAp (preparation conditions: CS/HAp with a volume ratio of 1 : 1, pH = 6.5, final sample contain 1.5 wt % CS).

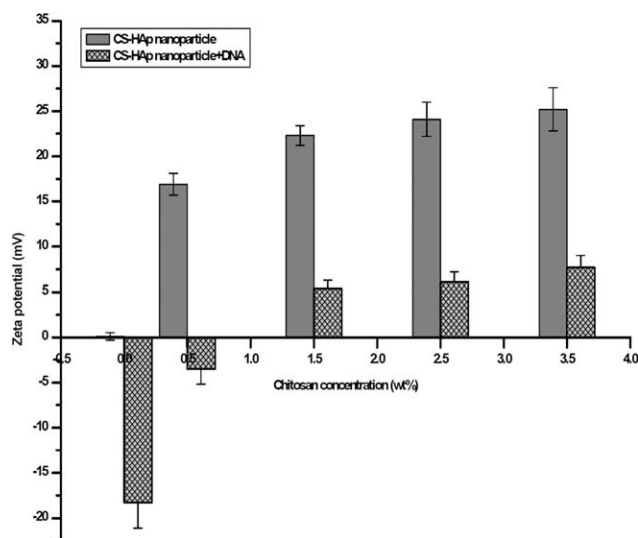


Figure 6 Effect of dispersed chitosan concentration on the zeta potential of CS-HAp nanoparticles (preparation condition: CS/HAp with a volume ratio of 1 : 1, pH = 6.5).

expression could take place. To facilitate the formation of nanoparticles-DNA complex through electrostatic attraction, we have employed chitosan to coat the surface of HAp nanoparticles to modulate the overall surface charge of these nanoparticles, so they could interact with DNA to produce nearly charge-neutral DNA-nanoparticle complexes.

Figure 6 shows that the ζ -potential of chitosan-coated HAp nanoparticle increased with chitosan feed concentrations until a ζ -potential plateau was reached at $\sim +25$ mV when produced in a chitosan concentration of ~ 2.5 – 3.5 wt %. It also found that as 1.5 wt % of chitosan was employed in conjunction with plasmid DNA (20 μ g), the zeta potentials of HAp-DNA nanoplexes transitioned from negative to positive charge. The positive ζ -potential of chitosan-coated HAp nanoparticles confirmed the presence of chitosan on HAp. The gradual increase of ζ -potential at low concentrations of chitosan indicated a gradual increase of surface chitosan until a steady surface charge was reached at high chitosan concentrations. The plateau in ζ -potential with increased initial chitosan could be indicative of saturated adsorption of chitosan on HAp nanoparticles. According to Tan et al.'s⁷ study, the continued adsorption of chitosan on nanoparticles did not affect the apparent zeta potential at high concentrations. Therefore, the chitosan concentration was fixed at 1.5 wt % for further biochemical study.

Coupling DNA to CS-HAp nanoparticles

By using an agarose gel electrophoresis technique, the ability of CS-HAp nanoparticles to interact with DNA was investigated. Figure 7 shows that no

retention is observed for free DNA (Lane 1). However, CS-HAp nanoparticles showed an ability couple DNA. This is due to electrostatic interaction between CS-HAp and DNA causing retardation of DNA in the well but not migration into the gel. In the electrophoresis experiments, cationic Lipofectin also showed an ability to retard the electrophoresis mobility of DNA. Agarose gel electrophoresis was also used to determine the rate of CS-HAp/DNA interaction. Results showed that the extent of DNA retardation in the sample well increased with the increasing ratio of CS-HAp/DNA. In this gel shift experiment, CS-HAp nanoparticles were made at the volume ratio 1 : 1 of CS/HAp. When the mass ratio of the CS-HAp/DNA was higher than 2 : 1, DNA was completely coupled with CS-HAp nanoparticles. This result indicates that these CS-HAp nanoparticles may serve as potential gene carriers for gene delivery.

Cell viability

Toxicity of gene vectors including viral vectors, cationic liposomes, and polymeric cations is a major barrier to efficient delivery of exogenous genes. In this study, the exponentially grown NIH3T3 cells and HeLa cells were treated with various amounts of CS-HAp nanoparticles ranging from 10 to 40 μ g, and the cell viability was measured by the MTT

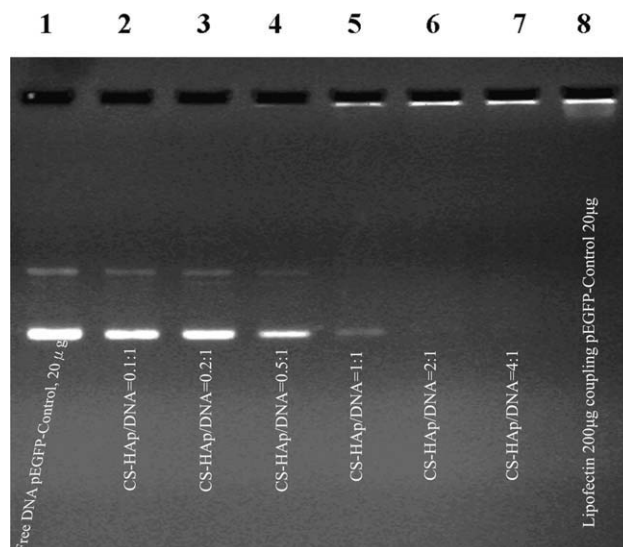


Figure 7 Gel retardation showing the coupling ability of CS-HAp nanoparticles for the coupling of plasmid DNA pEGFP-Control. Lane 1: Free DNA pEGFP-Control, 20 μ g; Lanes 2: CS-HAp/DNA = 0.1 : 1; Lane 3: CS-HAp/DNA = 0.2 : 1; Lanes 4: CS-HAp/DNA = 0.5 : 1; Lane 5: CS-HAp/DNA = 1 : 1; Lane 6: CS-HAp/DNA = 2 : 1; Lane 7: CS-HAp/DNA = 4 : 1; Lane 8: Lipofectin 200 μ g coupling pEGFP-Control 20 μ g (preparation condition: CS/HAp with a volume ratio of 1 : 1, pH = 6.5, final sample contain 1.5 wt % CS).

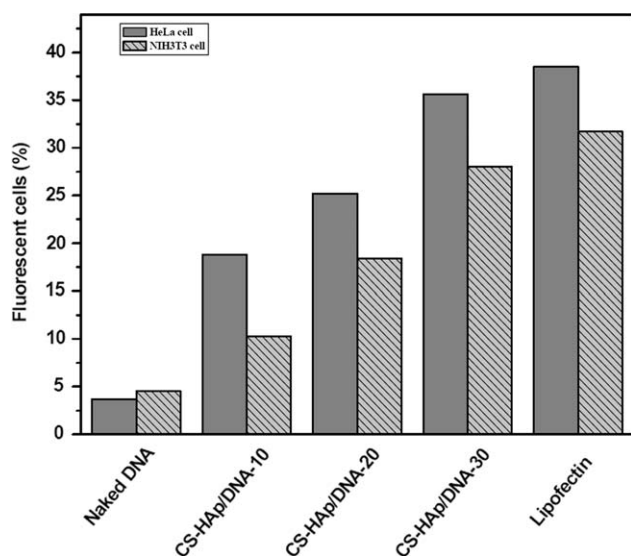


Figure 8 Flow cytometry of transfected HeLa and NIH3T3 cells by Naked DNA, CS-HAp/DNA-10, CS-HAp/DNA-20, CS-HAp/DNA-30 complexes and lipofectin. HeLa and NIH3T3 cells after transfection with 20 μ g of pEGFP were washed, trypsinized, and quantified using the FACS machine (-number: volumes of complexes (μ L)) (preparation condition: CS/HAp with a volume ratio of 1 : 1, pH = 6.5, final sample contain 1.5 wt % CS).

assay. Figure 8 shows the cytotoxicity of transfection vector in HeLa cell line and NIH3T3 cell line, respectively. The inhibition of cell viability by CS-HAp nanoparticles was clearly observed in a dose- and cell-dependent manner. CS-HAp was found to be less cytotoxic compared with lipofectin both in HeLa and NIH3T3 cell. Cells grew well even at the concentration as high as 30 μ g. The results further demonstrate that CS-HAp is a noncytotoxic, biocompatible, and safe vector.

Transfection and expression of the pEgfp plasmid coupled with the CS-HAp particles

To evaluate the effect of CS-HAp nanoparticle on transferring DNA, we investigated the transfection efficiency of complexes containing plasmid DNA in HeLa and NIH3T3 cells to find the gene expression level. The amount of CS-HAp in complexes used in this experiment was much less than 30 μ g, which would not affect the cell viability obviously according to the result mentioned in the cell viability assay. To determine the gene transfer capability of nanoparticles *in vitro* exactly, flow cytometry experiments were conducted to determine the pEGFP-N₂ transfection levels in HeLa and NIH3T3 cells. It was found that the number of green fluorescent cells for the cationic Lipofectin/DNA complexes increased in HeLa cells as well as NIH3T3 cells, which were a higher number compared with that of green fluorescent cells for the CS-HAp/DNA complexes (Fig. 9).

However, as the amount of CS-HAp nanoparticles increased, the transfection efficiency also increased. This demonstrated that the chitosan conjugation can minimize particle aggregation in buffers, especially in the transfection medium and improve the transfection efficiency of CS-HAp nanoparticles.

CONCLUSIONS

Nano-sized CS-HAp nanoparticles were synthesized successfully in aqueous solutions. The particle size is about 40–50 nm in width and 60–70 nm in length. It is an easy, inexpensive method to produce uniform nanoparticles with controllable average diameters in bulk quantities. It was found that the diameter of the CS-HAp nanoparticles could be easily controlled by the concentration of chitosan, the volume ratio of CS to HAp and the final pH of the suspension. By dropping HAp suspension (1 g HAp dissolved in 100 mL deionized water) into CS solution (1.5 g CS dissolved in diluting acetic solution) in a volume ratio of 1 : 1 at the pH 6.5 condition, CS-HAp nanoparticles can be obtained. Preliminary experiment shows that the nanoparticles was nontoxic and can bind plasmid DNA very well. Lipofectin/DNA complexes increased in HeLa cells as well as NIH3T3 cells, which were a higher number compared with that of CS-HAp/DNA complexes. However, such nanoparticles can be used as complementary technology to deliver gene vectors tailored for specific cell types.

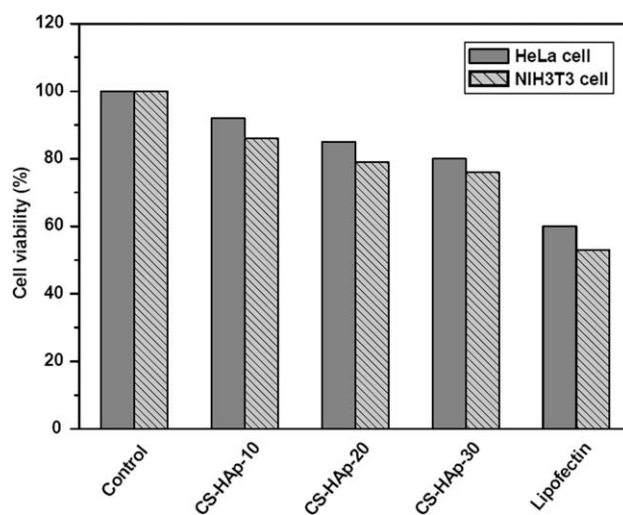


Figure 9 Biocompatibility of CS-HAp/DNA nanoparticles illustrated by lack of cellular toxicity on HeLa cells and NIH3T3 incubated with CS-HAp nanoparticle composed of different amount (10, 20, and 30 μ g). Lipofectin (10 μ g) was used in comparison. Cell viability is measured with the MTT assay and compared to non-treated cells, which are considered as 100% (preparation condition: CS/HAp with a volume ratio of 1 : 1, pH = 6.5, final sample contain 1.5 wt % CS).

References

1. Simon, R. H.; Engelhardt, J. F.; Yang, Y.; Zepeda, M.; Weber-Pendelton, S.; Grossman, M. J.; Wilson, M. *Hum Gene Ther* 1993, 4, 771.
2. Liu, F.; Huang, L. *J Control Release* 2002, 78, 259.
3. Brown, M. D.; Schätzlein, A. G.; Uchegbu, I. F. *Int J Pharm* 2001, 229, 1.
4. Bisht, S.; Bhakta, G.; Mitra, S.; Maitra, A. *Int J Pharm* 2005, 6, 288.
5. Kumta, P. N.; Sfeir, C.; Lee, D. H.; Olton, D.; Choi, D. *Acta Biomater* 2005, 1, 1.
6. Amarnath, M. *Expert Rev Mol Diagn* 2005, 13, 6.
7. Tan, K.; Cheang, P.; Ho, I. A. W.; Lam, P. Y. P.; Hui, K. M. *Gene Ther* 2007, 14, 828.
8. Choy, J. H. *Angew Chem Int Ed* 2000, 39, 4041.
9. Rolland, A. P. *Crit Rev Ther Drug Carrier Syst* 1998, 15, 143.
10. Janes, K. A.; Calvo, P.; Alonso, M. *J Adv Drug Deliv Rev* 2001, 47, 83.
11. Zhu, S. H.; Huang, B. Y.; Zhou, K. C. *J. Nanopart Res* 2004, 6, 307.
12. Olton, D.; Li, J. H.; Wilson, M. E. *Biomaterials* 2007, 28, 1267.
13. Ferraz, M. P.; Monteiro, F. J.; Manuel, C. M. *J Appl Biomater Biomech* 2004, 2, 74.
14. Jarcho, M.; Bolen, C. H.; Thomas, M. B.; Bobick, J.; Kay, J. F.; Doremus, R. H. *J Mater Sci* 1976, 11, 2027.
15. Shih, W. J.; Chen, Y. F.; Wang, M. C.; Hon, M. H. *J. Cryst Growth* 2004, 270, 211.
16. Suchanek, W.; Yoshimura, M. *J Mater Res* 1998, 13, 94.
17. Beppu, M. M.; Santana, C. C. *Key Eng Mater* 2001, 192, 31.
18. Yamaguchi, I.; Tokuchi, K.; Fukuzaky, H.; Koyama, Y.; Takakuda, K.; Momna, H.; Tanaka, J. *Key Eng Mater* 2001, 192, 673.
19. Rusu, V. M.; Ng, C. H.; Wilke, M.; Tiersch, B.; Fratzl, P.; Peter, M. G. *Biomaterials* 2005, 26, 5414.
20. Wilson Jr, O. C.; Hull, J. R. *Mater Sci Eng C Biol S* 2008, 28, 434.
21. Shih, W. J.; Wang, J. W.; Wang, M. C.; Hon, M. H. *Mater Sci Eng C Biol S* 2006, 26, 1434.
22. Degirmenbasi, N.; Kalyon, D. M.; Birinci, E. *Colloids Surf B Biointerface* 2006, 48, 42.
23. Fulmer, M. T.; Brown, P. W. *J Mater Sci Mater Med* 1998, 9, 197.
24. Han, Y.; Li, S.; Wang, X.; Bauer, I.; Yin, M. *Ultrason Sonochem* 2007, 14, 286.
25. Wu, Y.; Bose, S. *Langmuir* 2005, 21, 3232.
26. Cappelletti, G.; Bianchi, C. L.; Ardizzone, S. *Appl Surf Sci* 2006, 253, 519.
27. Yamaguchi, I.; Tokuchi, K.; Fukuzaky, H.; Koyama, Y.; Takakuda, K.; Momna, H.; Tanaka, J. *J Biomed Mater Res* 2001, 55, 20.
28. Murugan, R.; Ramakrishna, S. *Biomaterials* 2004, 25, 3829.
29. Chen, F.; Wang, Z. C.; Lin, C. *J Mater Lett* 2002, 57, 858.